Local adaptation and dispersal evolution interact to drive population response to climate change

Christopher Weiss-Lehman[1] and Allison K. Shaw[1]

[1]Ecology, Evolution, and Behavior, University of Minnesota

1 Introduction

Climate change is expected to dramatically reshape global biogeographic patterns as some species shift their ranges to track changing environmental conditions (Gonzalez et al., 2010; Peñuelas and Boada, 2003; Hansen et al., 2001; Scholze et al., 2006). These range shifts are generally predicted to proceed upwards in latitude, elevation, or both as average global temperatures continue to rise (Loarie et al., 2009). In fact, contemporary range shifts have already been observed in a wide range of taxa (Chen et al., 2011; Walther et al., 2002; Parmesan and Yohe, 2003; Parmesan, 2006; Parmesan et al., 1999; Perry et al., 2005). Such range shifts present significant challenges to current and future conservation efforts as they can result in both the extinction of populations failing to track a changing climate (Davis and Shaw, 2001; Parmesan, 2006; Zhu et al., 2012; Sekercioglu et al., 2008), and the creation of novel species assemblages as not all species shift their ranges at the same rate or at all (Hobbs et al., 2009; Gilman et al., 2010; Williams and Jackson, 2007), or both. It is therefore crucial to understand the dynamics of such climate-induced range shifts to better inform current and future conservation work.

While the study of range shifts due to climate change is relatively new, important insights can be gained from the related but distinct process of range expansion. Range expansions have been studied for decades, leading to a robust understanding of both the ecological (Skellam, 1951; Hastings et al., 2005) and evolutionary (Shine et al., 2011; Burton et al., 2010; Excoffier et al., 2009; Kubisch et al., 2014) mechanisms responsible for shaping such expansions. For example,

while the speed of a range expansion can be well approximated by a combination of the species' intrinsic growth rate and dispersal ability (Hastings et al., 2005), recent research demonstrates that evolution in both of these traits can have important implications for both the mean and variance of expansion speed through time (Weiss-Lehman et al., 2017; Ochocki and Miller, 2017; Szűcs et al., 2017; Phillips, 2015; **?**). Since range shifts, like range expansions, have a leading edge of population advance, they are likely to be affected by similar ecological and evolutionary mechanisms as have been shown to drive dynamics in range expansions (Hargreaves and Eckert, 2014). However, while such insights from range expansions are valuable for understanding and predicting dynamics of range shifts, it is important to recognize that these two processes have significant differences as well.

In particular, range expansions and range shifts due to climate change involve fundamentally distinct initial conditions. Range expansions, especially for invasive and reintroduced species, typically begin from the successful establishment and subsequent spread of a small, founding population (Hastings et al., 2005). Such founding populations often represent samples from some larger source population and as such lack any initial spatial population structure. In contrast, range shifts start from entire populations with existing spatial structure within the initially stable range (Hargreaves and Eckert, 2014). Such spatial structure can take the form of local adaptation within the range, the severity of the gradient in population size from the range core to edge, or some combination of the two (Hargreaves and Eckert, 2014; Hargreaves et al., 2015; Henry et al., 2013).

These different aspects of spatial population structure have been shown to dramatically impact the response of populations to climate change. For example, the mechanism responsible for the gradient in population size from core to edge (e.g. declines in birth rates vs. increases in extinction risk) can directly change the probability of extinction a species faces during a climate driven range shift (Henry et al., 2013). A population's risk of extinction during a range shift has also been related to local adaptation within the range. Specifically, a broad environmental niche (i.e. little local adaptation) can decrease a population's ability to track a changing climate if dispersal occurs in a stepping stone manner, allowing some individuals to block dispersal of better adapted phenotypes (Atkins and Travis, 2010). Local adaptation also has the potential to interact with dispersal

evolution during climate change, driving increased dispersal probability in an asexual species as genotypes shift to keep pace with their environmental optimum (Hargreaves et al., 2015). However, it is unclear how dispersal evolution and local adaptation might interact in a sexually reproducing species in which dispersal and fitness are directly linked via gene flow. For example, evolution of increased dispersal could simultaneously reduce local adaptation within a population due to increased gene flow throughout the range. In fact, long-distance pollen dispersal in flowering plants has been shown to restrict local adaptation and, when pollen dispersal sufficiently outpaces seed dispersal, to lead to ecological niche shifts, rather than spatial range shifts, in response to simulated climate change (Aguilée et al., 2016). Additionally, the distribution of dispersal phenotypes within a population can be influenced by the severity of the gradient at the range edge (Henry et al., 2013; Hargreaves and Eckert, 2014), further complicating the relationship between dispersal evolution and local adaptation during climate-induced range shifts. Evolution during range shifts due to local adaptation and dispersal evolution are both potentially important drivers of range shift dynamics (Van Petegem et al., 2016) and it is therefore important to consider both when predicting the dynamics of populations responding to climate change.

Here, we develop a complex, individual-based model of a sexually reproducing species, which incorporates evolution in both fitness (via local adaptation) and dispersal distance to determine the interaction between the strength of local selection and the starkness of the gradient at the range edge in driving population dynamics during climate change. Using this model, we simultaneously vary the strength of local selection and the starkness of the range boundary to ascertain the relationship between them and test how dispersal evolution interacts with local adaptation to help or hinder a population's ability to track a changing climate. We additionally compare the dynamics of successful versus doomed simulated populations to understand the factors contributing to population extinction during climate-induced range shifts.

2 Methods

2.1 Overview

2.1.1 Purpose

This model tests an evolving population's ability to track a changing climate under a variety of conditions. Specifically, populations are simulated under different combinations of (1) the starkness of the range boundary and (2) the strength of local selection. In all simulations, individual dispersal and relative fitness are defined by an explicit set of quantitative diploid loci subject to mutation, thus allowing both traits to evolve over time. All simulations begin with stable climate conditions for 2000 generations to allow the populations to reach a spatial equilibrium before the onset of climate change. Climate change is then modeled as a constant, directional shift in the location of environmentally suitable habitat (see the *Submodels* section below). Finally, simulations end with another short period of climate stability to assess the population's ability to persist and recover after shifting its range.

2.1.2 State variables and scales

The model simulates a population of male and female individuals characterized by spatial coordinates for their location and by diploid loci for both fitness and dispersal. Space is modeled as a lattice of discrete patches overlaying a continuous Cartesian coordinate system with a fixed width along the y axis and without bounds on the x axis. To avoid edge effects along the y axis, the model employs wrapping boundaries such that if an individual disperses out of the landscape on one side, it appears at the opposite end of the same row of the landscape. Patches are defined by the location of the patch center in x and y coordinates and a patch width parameter defining the relationship between continuous Cartesian space and the discrete patches used for population dynamics (see the *Submodels* section below).

The abiotic environment is defined by the location of the center of the range, the slope of the range boundary, and the width of the range (See Figure 1). The range can then shift in space by altering the location of the range center, which is how climate change is implemented in the

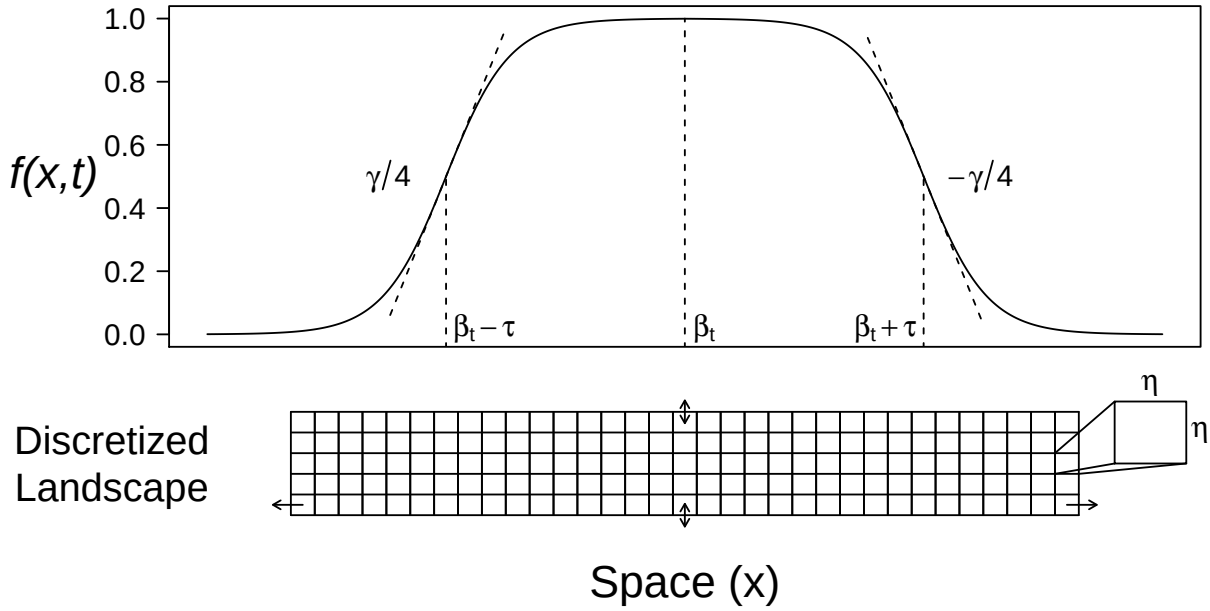

Figure 1: Environmental quality, as defined by $f(x,t)$, over a spatial gradient. The parameters of $f(x,t)$ are shown on the figure at significant points along the x axis. Additionally, the lattice of discrete patches in which population dynamics occur is shown beneath. This lattice of η x η patches are mapped to environmental conditions along the x axis using $f(x,t)$ and are environmentally constant along the y axis. Dispersal is unbounded in the x direction and implemented with wrapping boundaries in the y direction.

model. Further, a gradient of phenotypic optimum values for fitness is imposed within the range to allow for local adaptation within the range boundaries. The severity of this gradient is defined independently of the other environmental parameters.

2.1.3 Process overview and scheduling

Time is also modeled in discrete intervals defining single generations of the population. Within each generation, individuals first disperse from their natal patches according to their dispersal phenotypes (*Submodels*). After dispersal, reproduction occurs according to a stochastic implementation of the classic Ricker model (Ricker, 1954) taking into account the mean fitness of individuals within the patch (*Submodels*). Parental pairs form via random sampling of the local population (with replacement) weighted by individual fitness such that individuals with high fitness are likely to produce multiple offspring while individuals with no fitness may not produce any. Individuals

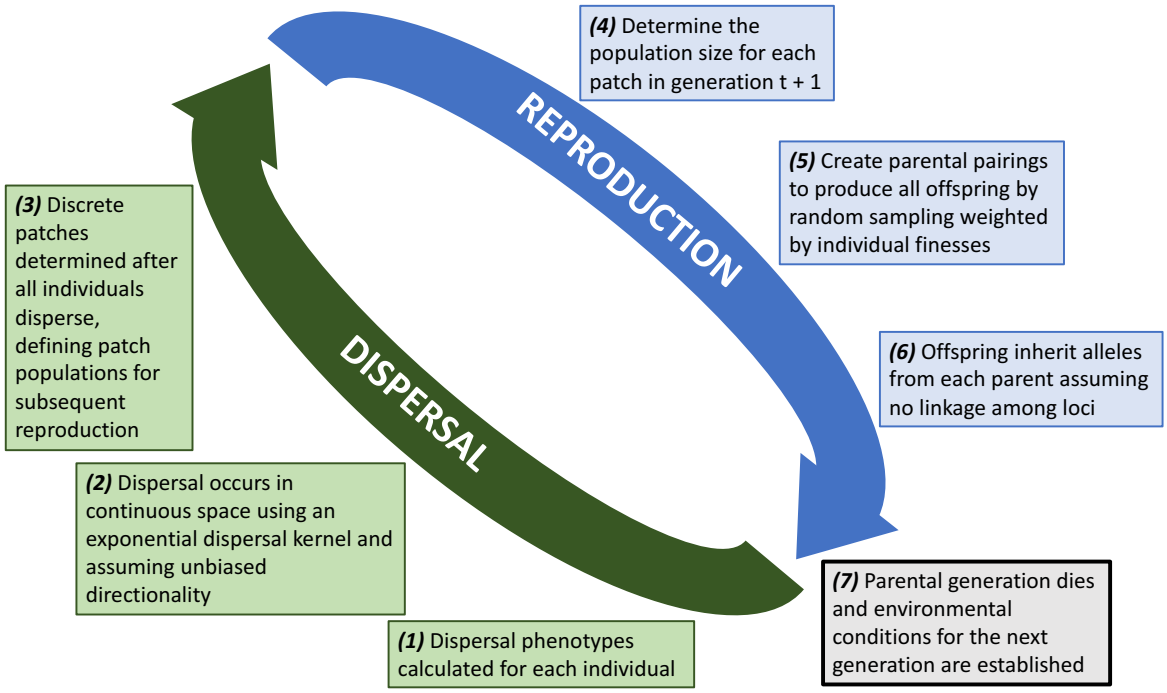

Figure 2: The life cycle of simulated populations is shown divided between events contributing to reproduction and dispersal. Each generation begins with new offspring dispersing according to their phenotype, after which reproduction occurs in local populations defined by the discrete lattice. After reproduction, all parental individuals perish, resulting in discrete, non-overlapping generations.

inherit one allele from each parent at each loci, assuming independent segregation and a mutation process (*Submodels*). After reproduction, all individuals in the current generation perish and the offspring begin the next generation with dispersal, resulting in discrete, non-overlapping generations.

2.2 Design concepts

2.2.1 Emergence

Emergent phenomena in this model include the spatial equilibrium of population abundances and trait values within the stable range, the demographic dynamics of the shifting population during climate change, and the evolutionary trajectories of both fitness and dispersal traits during climate change. These are all examined in the context of their impact on the population's ability to keep

pace with the changing climate.

2.2.2 Stochasticity

All biological processes in this model are stochastic including realized population growth in each patch, dispersal distances of each individual, and inheritance of loci. Environmental parameters are fixed, however, and the process of climate change (i.e. the movement of environmentally suitable habitat through time) is deterministic. Thus, the model removes the confounding influence of environmental stochasticity to focus on demographic and evolutionary dynamics of range shifts.

2.2.3 Interactions

Individuals in the model interact via mating and density-dependent competition within patches. Other important interactions are the relationship between dispersal evolution and local adaption, particularly in edge populations, and how this relationship impacts a population's ability to avoid extinction and track a changing climate. These interactions are examined in the context of different configurations of the initial, stable range and different speeds of climate change.

2.2.4 Desired output

After each model run, full details of all surviving individuals at the last time point are recorded (spatial coordinates and loci values for both traits). If a population went extinct during the model run, the time of extinction is recorded. Throughout the simulation, certain aggregated values are calculated and recorded for each occupied patch including the population size and the mean and variance of allele values for each trait.

2.3 Details

2.3.1 Initialization

The following parameters are set at the beginning of each simulation and form the initial conditions of the model: the mean and variance for allele values of each trait, population size, location of environmentally suitable habitat, number of generations for the pre-, post-, and during climate

change periods of the simulation, and all other necessary parameters for the submodels defined below. Simulated populations are initialized in the center of the range and allowed to spread and equilibrate throughout the range during the period of stable climate conditions. This ensures that the populations reacting to a changing climate truly represent the expected spatial distribution for a given range, rather than the initial parameter values used in the simulation. See Table 1 for a full list of all parameter values used in the simulations described here.

2.3.2 Submodels

Environmentally suitable habitat Environmentally suitable habitat is determined by the population's carrying capacity as it ranges in space (K_x). The carrying capacity is maximized in the center of the species' range (K_{max}) and declines with increasing distance from the center. Specifically, the carrying capacity at a location x is defined as the product of K_{max} and a function $f(x,t)$, where $f(x,t)$ ranges from 1 in the range center to 0 far away from the center and is defined as follows

$$f(x,t) = \begin{cases} \frac{e^{\gamma(x-\beta_t+\tau)}}{1+e^{\gamma(x-\beta_t+\tau)}} & x \leq \beta_t \\ \frac{e^{-\gamma(x-\beta_t-\tau)}}{1+e^{-\gamma(x-\beta_t-\tau)}} & x > \beta_t \end{cases} \tag{1}$$

where β_t defines the center of the area of suitable habitat at time t, τ sets the width of the range, and γ affects the slope of the function at the range boundaries (See Figure 1). To understand the relationship between γ and the slope of $f(x,t)$ at the range boundary, the partial derivative of $f(x,t)$ over the spatial dimension can be shown to be

$$f(x,t) = \begin{cases} \frac{\gamma e^{\gamma(x-\beta_t+\tau)}}{(1+e^{\gamma(x-\beta_t+\tau)})^2} & x \leq \beta_t \\ \frac{-\gamma e^{-\gamma(x-\beta_t-\tau)}}{(1+e^{-\gamma(x-\beta_t-\tau)})^2} & x > \beta_t \end{cases} \tag{2}$$

yielding a derivative of $\pm\frac{\gamma}{4}$ at the inflection points on either side of the range center ($x = \beta_t \pm \tau$).

Population dynamics occur within discrete patches, so to calculate a K_x value for a discrete patch from the continuous function $f(x,t)$, we use another parameter defining the spatial scale of each patch (η; See Figure 1). The local carrying capacity of a patch centered on x (K_x) is then

calculated as the mean of $f(x,t)$ over the interval of the patch multiplied by K_{max}.

$$K_x = \frac{K_{max}}{\eta} \int_{x-\frac{\eta}{2}}^{x+\frac{\eta}{2}} f(x,t)dx \tag{3}$$

By varying the parameters defining $f(x,t)$, we can change both the total achievable carrying capacity of the population throughout the range (by altering both τ and γ) and the slope at which K_x declines to 0 (by altering γ). Changing the slope affects not only the rate at which K_x declines at the range boundaries (our focus), but it also alters the total achievable carrying capacity of the population. To avoid this confounding factor, we fix the total area under the curve $f(x,t)$. The indefinite integral of $f(x,t)$ can be shown to be

$$\int_{-\infty}^{\infty} f(x,t)dx = \frac{2ln(e^{\gamma\tau}+1)}{\gamma} \tag{4}$$

which can be solved for τ. For a given fixed total area under the curve, an appropriate value of τ can be calculated for each value of γ.

Thus, γ and τ are both fixed within a given simulation and β_t (the location of the center of suitable habitat) is used to simulate climate change. During the periods before and after climate change β_t is constant, but to simulate climate change it varies with time as follows

$$\beta_t = \nu\eta(t-\hat{t}) \tag{5}$$

where ν is the velocity of climate change per generation in terms of discrete patches, η is the spatial scale of each patch, t is the current generation, and $\hat{t}$ is the last generation of stable climatic conditions before the onset of climate change.

Local adaptation To allow an arbitrary degree of local adaptation within the range, the local phenotypic optima ($z_{opt,x}$) is set as follows

$$z_{opt,x} = \lambda(x-\beta_t) \tag{6}$$

where λ defines the strength of local selection with values close to 0 resulting in little to no change in phenotypic optimum across the range and values of greater magnitude resulting in large differences in phenotypic optima across the range. Individual fitness ($w_{i,x}$) values are then calculated according to the following equation assuming stabilizing selection

$$w_{i,x} = e^{\frac{-(z_i - z_{opt,x})^2}{2\omega^2}} \tag{7}$$

where ω defines the strength of stabilizing selection and z_i is an individual's fitness phenotype (Lande, 1976). All loci are assumed to contribute additively to the phenotype with no dominance or epistasis, meaning an individual's phenotype is simply the sum of the individual's allele values for the fitness trait.

Population dynamics Population growth within each patch is modeled with a stochastic implementation of the classic Ricker model (Ricker, 1954; Melbourne and Hastings, 2008). To account for fitness effects on population growth, expected population growth is scaled by the mean relative fitness of individuals within the patch ($\bar{w_x}$). The expected number of new offspring in patch x at time $t+1$ is then given by

$$\hat{N}_{t+1,x} = \bar{w_x} F_{t,x} \frac{R}{\psi} e^{\frac{-RN_{t,x}}{K_x}} \tag{8}$$

where $F_{t,x}$ is the number of females in patch x at time t, R is the intrinsic growth rate for the population, ψ is the expected sex ratio of the population, $N_{t,x}$ is the number of individuals (males and females) in patch x at time t, and K_x is the local carrying capacity based on the environmental conditions. To incorporate demographic stochasticity, the realized number of offspring for each patch is then drawn from a Poisson distribution.

$$N_{t+1,x} \sim Poisson(\hat{N}_{t+1,x}) \tag{9}$$

Parentage of the offspring is then assigned by random sampling of the local male and female population (i.e. polygynandrous mating). The sampling is weighted by individual fitness and occurs with replacement so highly fit individuals are likely to have multiple offspring while low

fitness individuals may not have any. Each offspring inherits one allele per locus from each parent, assuming no linkage among loci. After reproduction, all members of the previous generation die and the offspring disperse to begin the next generation.

Mutation Inherited alleles are subject to mutation such that some offspring might not inherit identical copies of certain alleles from their parents. The mutation process is defined by two parameters for each trait T: the diploid mutation rate (U^T) and the mutational variance (V_m^T). Using these parameters along with the number of loci defining trait T (L^T), the per locus probability of a mutation is

$$\frac{U^T}{2L^T} \tag{10}$$

Mutational effects are drawn from a normal distribution with mean 0 and a standard deviation of

$$\sqrt{V_m^T U^T} \tag{11}$$

By defining the mutation process in this manner rather than setting a probability of mutation and mutational effect directly, similar mutational dynamics can be imposed regardless of the number of loci used in the simulation.

Dispersal Finally, individuals disperse according to an exponential dispersal kernel defined by each individual's dispersal phenotype. An individual's dispersal phenotype is the expected dispersal distance and is given by

$$d_i = \frac{D\eta e^{\rho \Sigma L^D}}{1 + e^{\rho \Sigma L^D}} \tag{12}$$

where D is the maximum expected dispersal distance in terms of discrete patches, η is the spatial scale of discrete patches, ρ is a constant determining the slope of the transition between 0 and D, and the summation is taken across all alleles contributing to dispersal. Thus, as with fitness, loci are assumed to contribute additively with no dominance or epistasis. The expected dispersal distance, d_i is then used to draw a realized distance from an exponential dispersal kernel. The direction of dispersal is drawn from a uniform distribution bounded by 0 and 2π. If a dispersal

trajectory takes an individual outside the bounds of the landscape in the y axis, the individual reappears at the same x coordinate but the opposite end of the y axis, thus wrapping the top and bottom edges of the landscape to avoid edge effects. Dispersal occurs from the center of each patch and the individual's new patch is then determined according to its location in the overlaid grid of η x η patches (see Figure 1).

2.4 Simulation descriptions

Most of the parameters described above were held constant over all simulations we performed (Table 1). We varied certain parameter values to explore the interacting roles of local adaptation, the habitat gradient at the range edge, and the speed of climate change in the dynamics of range shifts. Specifically, we considered a factorial combination of three severities of habitat quality decline at the range edge, three degrees of local adaptation within the range, and three speeds of climate change (Table 2) for a total of 27 different model scenarios. For each scenario, we performed 100 simulations to assess the interacting ecological and evolutionary dynamics of climate driven range shifts. All simulations were performed in R version 3.4.4 (Team, 2000) and the code is available at `https://github.com/tpweiss06/ShiftingSlopes`.

References

Aguilée, R., G. Raoul, F. Rousset, and O. Ronce. 2016. Pollen dispersal slows geographical range shift and accelerates ecological niche shift under climate change. Proceedings of the National Academy of Sciences 113:E5741–E5748.

Atkins, K., and J. Travis. 2010. Local adaptation and the evolution of species? ranges under climate change. Journal of Theoretical Biology 266:449–457.

Burton, O. J., B. L. Phillips, and J. M. Travis. 2010. Trade-offs and the evolution of life-histories during range expansion. Ecology Letters 13:1210–1220.

Chen, I.-C., J. K. Hill, R. Ohlemüller, D. B. Roy, and C. D. Thomas. 2011. Rapid range shifts of species associated with high levels of climate warming. Science 333:1024–1026.

Parameter	Description	Value
N_1	Initial population size (seeded across multiple patches) when beginning the simulations	2500
β_1	Center of environmentally suitable habitat before climate change	0
η	Spatial dimensions of habitat patches in continuous space	50
y_{max}	Number of patches the discrete lattice extends in the y direction	10
$\hat{t}$	Last time point of stable climate conditions	2000
t_Δ	Duration of climate change	100
t_{max}	Total number of time points in the simulation	2150
R	Intrinsic growth rate of the population	2
K_{max}	Maximum achievable carrying capacity in the range	100
ψ	Expected sex ratio in the population	0.5
D	Maximum achievable dispersal phenotype	1000
ρ	Determines the slope of the transition in dispersal phenotypes from 0 to D	0.5
ω	Defines the strength of stabilizing selection on fitness traits	3
U^T	Diploid mutation rate for each trait	0.02 for each trait
V_m^T	Mutational variance for each trait	0.0004 for each trait
L^T	The number of diploid loci defining each trait	5 for each trait
μ_1^f	The initial mean allele value for the fitness trait	0
μ_1^d	The initial mean allele value for the dispersal trait	-1
σ_1^f	The initial standard deviation of allele values for fitness	0.025
σ_1^d	The initial standard deviation of allele values for dispersal	1

Table 1: Simulation parameters held constant across all scenarios presented here.

Habitat gradient at range edge	Strength of local adaptation	γ	τ	λ
Shallow	None	0.0025	250	0
	Moderate	0.0025	250	0.004
	Strong	0.0025	250	0.008
Moderate	None	0.025	421.479	0
	Moderate	0.025	421.479	0.004
	Strong	0.025	421.479	0.008
Stark	None	0.25	421.48	0
	Moderate	0.25	421.48	0.004
	Strong	0.25	421.48	0.008

Table 2: Descriptions and parameter values for the 9 different scenarios examined here. For each scenario, ν (the speed of climate change) was varied among 0.5, 1, and 2.

Davis, M. B., and R. G. Shaw. 2001. Range shifts and adaptive responses to quaternary climate change. Science 292:673–679.

Excoffier, L., M. Foll, and R. J. Petit. 2009. Genetic consequences of range expansions. Annual Review of Ecology, Evolution, and Systematics 40:481–501.

Gilman, S. E., M. C. Urban, J. Tewksbury, G. W. Gilchrist, and R. D. Holt. 2010. A framework for community interactions under climate change. Trends in ecology & evolution 25:325–331.

Gonzalez, P., R. P. Neilson, J. M. Lenihan, and R. J. Drapek. 2010. Global patterns in the vulnerability of ecosystems to vegetation shifts due to climate change. Global Ecology and Biogeography 19:755–768.

Hansen, A. J., R. P. Neilson, V. H. Dale, C. H. Flather, L. R. Iverson, D. J. Currie, S. Shafer, R. Cook, and P. J. Bartlein. 2001. Global change in forests: Responses of species, communities, and biomes: Interactions between climate change and land use are projected to cause large shifts in biodiversity. AIBS Bulletin 51:765–779.

Hargreaves, A., S. Bailey, and R. A. Laird. 2015. Fitness declines towards range limits and local

adaptation to climate affect dispersal evolution during climate-induced range shifts. Journal of evolutionary biology 28:1489–1501.

Hargreaves, A. L., and C. G. Eckert. 2014. Evolution of dispersal and mating systems along geographic gradients: implications for shifting ranges. Functional Ecology 28:5–21.

Hastings, A., K. Cuddington, K. F. Davies, C. J. Dugaw, S. Elmendorf, A. Freestone, S. Harrison, M. Holland, J. Lambrinos, U. Malvadkar, et al. 2005. The spatial spread of invasions: new developments in theory and evidence. Ecology Letters 8:91–101.

Henry, R. C., G. Bocedi, and J. M. Travis. 2013. Eco-evolutionary dynamics of range shifts: elastic margins and critical thresholds. Journal of Theoretical Biology 321:1–7.

Hobbs, R. J., E. Higgs, and J. A. Harris. 2009. Novel ecosystems: implications for conservation and restoration. Trends in ecology & evolution 24:599–605.

Kubisch, A., R. D. Holt, H.-J. Poethke, and E. A. Fronhofer. 2014. Where am i and why? synthesizing range biology and the eco-evolutionary dynamics of dispersal. Oikos 123:5–22.

Lande, R. 1976. Natural selection and random genetic drift in phenotypic evolution. Evolution 30:314–334.

Loarie, S. R., P. B. Duffy, H. Hamilton, G. P. Asner, C. B. Field, and D. D. Ackerly. 2009. The velocity of climate change. Nature 462:1052.

Melbourne, B. A., and A. Hastings. 2008. Extinction risk depends strongly on factors contributing to stochasticity. Nature 454:100.

Ochocki, B. M., and T. E. Miller. 2017. Rapid evolution of dispersal ability makes biological invasions faster and more variable. Nature communications 8:14315.

Parmesan, C. 2006. Ecological and evolutionary responses to recent climate change. Annu. Rev. Ecol. Evol. Syst. 37:637–669.

285 Parmesan, C., N. Ryrholm, C. Stefanescu, J. K. Hill, C. D. Thomas, H. Descimon, B. Huntley,
286 L. Kaila, J. Kullberg, T. Tammaru, et al. 1999. Poleward shifts in geographical ranges of butterfly
287 species associated with regional warming. Nature 399:579.

288 Parmesan, C., and G. Yohe. 2003. A globally coherent fingerprint of climate change impacts across
289 natural systems. Nature 421:37.

290 Peñuelas, J., and M. Boada. 2003. A global change-induced biome shift in the montseny mountains
291 (ne spain). Global change biology 9:131–140.

292 Perry, A. L., P. J. Low, J. R. Ellis, and J. D. Reynolds. 2005. Climate change and distribution
293 shifts in marine fishes. science 308:1912–1915.

294 Phillips, B. L. 2015. Evolutionary processes make invasion speed difficult to predict. Biological
295 Invasions 17:1949–1960.

296 Ricker, W. E. 1954. Stock and recruitment. Journal of the Fisheries Board of Canada 11:559–623.

297 Scholze, M., W. Knorr, N. W. Arnell, and I. C. Prentice. 2006. A climate-change risk analysis for
298 world ecosystems. Proceedings of the National Academy of Sciences 103:13116–13120.

299 Sekercioglu, C. H., S. H. Schneider, J. P. Fay, and S. R. Loarie. 2008. Climate change, elevational
300 range shifts, and bird extinctions. Conservation biology 22:140–150.

301 Shine, R., G. P. Brown, and B. L. Phillips. 2011. An evolutionary process that assembles phenotypes
302 through space rather than through time. Proceedings of the National Academy of Sciences
303 108:5708–5711.

304 Skellam, J. G. 1951. Random dispersal in theoretical populations. Biometrika 38:196–218.

305 Szűcs, M., M. Vahsen, B. Melbourne, C. Hoover, C. Weiss-Lehman, and R. Hufbauer. 2017. Rapid
306 adaptive evolution in novel environments acts as an architect of population range expansion.
307 Proceedings of the National Academy of Sciences 114:13501–13506.

308 Team, R. C. 2000. R language definition. Vienna, Austria: R foundation for statistical computing.
309 .

Van Petegem, K. H., J. Boeye, R. Stoks, and D. Bonte. 2016. Spatial selection and local adaptation jointly shape life-history evolution during range expansion. The American Naturalist 188:485–498.

Walther, G.-R., E. Post, P. Convey, A. Menzel, C. Parmesan, T. J. Beebee, J.-M. Fromentin, O. Hoegh-Guldberg, and F. Bairlein. 2002. Ecological responses to recent climate change. Nature 416:389.

Weiss-Lehman, C., R. A. Hufbauer, and B. A. Melbourne. 2017. Rapid trait evolution drives increased speed and variance in experimental range expansions. Nature communications 8:14303.

Williams, J. W., and S. T. Jackson. 2007. Novel climates, no-analog communities, and ecological surprises. Frontiers in Ecology and the Environment 5:475–482.

Zhu, K., C. W. Woodall, and J. S. Clark. 2012. Failure to migrate: lack of tree range expansion in response to climate change. Global Change Biology 18:1042–1052.